Proceedings of the ASME 2011 Pressure Vessels & Piping Division
PVP2011
July 17-21, 2011, Baltimore, Maryland, USA

PVP2011-57625

COMBINING CFD DERIVED INFORMATION AND THERMODYNAMIC ANALYSES TO INVESTIGATE WASTE HEAT BOILER CHARACTERISTICS

Sean M. McGuffie, P.E.
Porter McGuffie, Inc.
Lawrence, KS, USA
sean@pm-engr.com

Michael A. Porter, P.E.
Porter McGuffie, Inc.
Lawrence, KS, USA
mike@pm-engr.com

Dennis H. Martens, P.E.
Porter McGuffie, Inc.
Lawrence, KS, USA
martensdh@pm-engr.com

Michael J. Demskie
Flint Hills Resources
Pine Bend, MN, USA
Mike.Demskie@fhr.com

ABSTRACT

A series of computational fluid dynamics (CFD) and numerical analyses were performed to investigate operational characteristics in a sulfur recovery unit waste heat boiler (WHB). Similar analyses of WHBs have been reported by the authors (Porter et. al. [1, 2]). The initial focus for the current investigation was to determine the reason for metal loss on the inside of the tube. This required extending the focus of the previous analyses that concerned a) the departure from nucleate boiling (DNB) leading to critical tube temperatures, and b) the downstream fluxes and temperatures from the inlet ferrule, to also investigate high inside surface temperatures of the tubes caused by shell-side tube outer diameter (OD) fouling. The results of the investigations were combined to provide future operational guidance for the boiler.

As in the previously reported analyses, CFD submodels of the WHB process-side inlet were constructed and analyzed to determine the fluxes and temperatures that occur during several operational conditions. Queried results of these analyses were combined with the WHB's historical operational data to predict the nominal operational temperatures, and associated corrosion rates on the inner diameter (ID) of the tube.

A second set of submodels was used to determine inside tube operating temperatures resulting from external fouling. The queried results of these analyses were combined, using an expansion of standard thermodynamic analysis techniques, to study possible fouling regimes based on the standard fouling growth equation. Additionally, a 3-dimensional CFD analysis was conducted on the shell-side of the boiler. This analysis allowed the determination of the margin of safety (MOS) from a fall-off-the-cliff (FOC) event [1].

The results of the submodels, numerical analyses and the 3D shell-side analysis of the boiler were combined to determine operational limit curves for the boiler that were based on measurable process parameters including mass flow rate and thermal reactor temperature.

It should be noted that the procedures and analyses detailed in this paper do not comprise the complete analyses performed to qualify the past performance of the boiler and to determine future boiler operational limits. Additionally, due to the proprietary nature of the investigations, the specific numerical values related to the boiler's operation are not presented. Only the derivation of the equations and logic associated with the investigation and the derivation of operational guidance are given. Complete engineering to determine these limits requires additional analyses not detailed in this paper.

INTRODUCTION

WHBs are used downstream of Claus Reaction Furnaces (CRFs) in sulfur recovery units. The thermal reaction used to recover elemental sulfur occurs in the CRF. The primary Claus reactions are (Siemens [3]):

$$H_2S + \frac{3}{2}O_2 \rightarrow SO_2 + H_2O$$
$$2H_2S + SO_2 \rightarrow \frac{3}{2}S_2 + 2H_2O \quad (1)$$

The Claus thermal reactions occur when the acid gas is reacted with air, often with oxygen enhancement, in the thermal reactor. The reactions always occur at sub-stoichiometric fuel-to-air ratios as later catalyst beds are sensitive to free O_2 in the process stream. The reactions are extremely exothermic, resulting in gas temperatures in the range of 2200 – 2800 °F. The WHB is used to cool the gas before it enters the primary condenser for extraction of liquid elemental sulfur. The WHB also produces a byproduct of steam, typically 500 – 650 psig, for plant use. Due to the sub-stoichiometric chemistry involved, the reaction does not complete. This results in a typical H_2S content of 3 – 5 %Mol for the gas entering the WHB.

Steel exposed to high temperature gas containing H_2S will undergo sulfidation corrosion. Sulfidation results in the formation of an iron sulfide scale. This scale is brittle and results in a loss of the steel's mechanical integrity. The loss of mechanical integrity can lead to failures in the tubes and at the tube-to-tubesheet welds. These failures typically result in unanticipated plant shutdowns.

The rate of sulfidation is typically characterized by a relationship between process gas H_2S content and the exposed metal surface temperature. In industry, a Couper-Gorman type curve is used to estimate the corrosion rate in mils per year. Based on the authors' industrial experience, a modified curve was used to evaluate metal loss conditions for these investigations. This curve is shown in Figure 1.

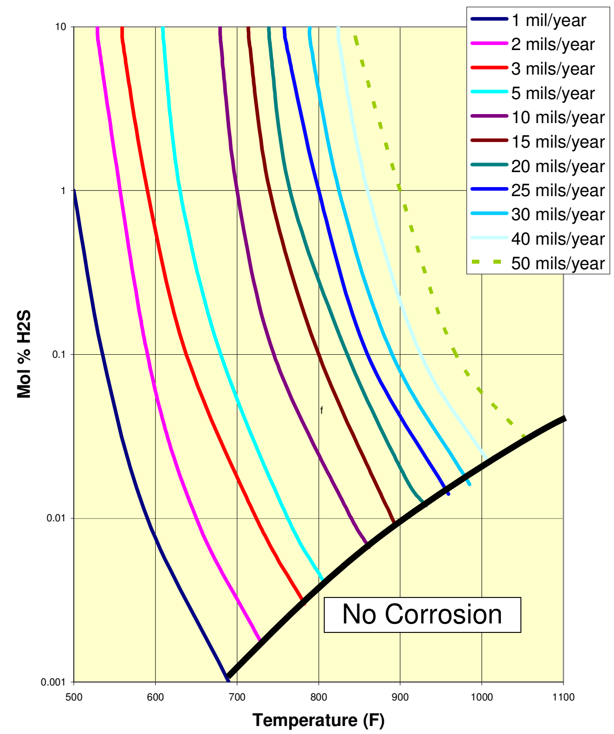

FIGURE 1 – AUTHORS' PROPOSED SULFIDATION CORROSION CURVE FOR CARBON STEEL

Operational experience indicates that acceptable rates of sulfidation corrosion occur when the design calculated maximum WHB tube metal temperature is less than or equal to 600 °F.

The WHB under consideration is a kettle type boiler with 355 tubes. The boiler was replaced in-kind in 2000. Eddy current inspection of the tubes in 2009 indicated that significant metal loss had occurred, resulting in a loss of approximately half of the tube material (~80 mils). This corrosion occurred directly downstream from the ferrules over a 2-3" area on the ID of the tubes. Figure 2 shows typical corrosion found upon removal for retubing.

FIGURE 2 – TYPICAL CORROSION OCCURRING DOWNSTREAM FROM FERRULE

It was determined that this level of material loss could be significant enough to precipitate mechanical failure of the tubes. For this reason the tubes were replaced. In addition to replacing the tubes, new multi-piece inlet ferrule assemblies were installed in the boiler.

For this project, the authors were tasked with determining the cause for the metal loss. The evaluation of a possible FOC event or external fouling events was necessary to establish the root cause for the metal loss. In addition, the task included making recommendations for future boiler operation, including developing an operational limit curve for the boiler based on the relevant parameters to avoid future metal loss. Development of the limit curve required a) investigating the previous in-service corrosion, b) extrapolating the results of this investigation to predict the corrosion performance of the retubed WHB, c) relating the results of the FOC analysis to the limit curve, and d) conducting additional investigations as required.

NOMENCLATURE

k-ε	=	Two-equation Reynolds averaged Navier Stokes (RANS) turbulence model
Y+	=	u^*y/ν, used in defining the law of the wall, a CFD specific variable (Adapco [4])
u^*	=	Friction velocity
y	=	Distance to nearest wall
ν	=	Local kinematic viscosity
MMSCFD	=	Millions of standard cubic feet per day
MMACFD	=	Millions of actual cubic feet per day
$m(t)$	=	Mass growth of fouling as a function of time
κ	=	Deposition rate constant
ρ	=	Fluid density
λ_c	=	Consolidation rate constant – shown as Lc in plots
λ_r	=	Re-entrainment rate constant – shown as Lr in plots
λ	=	$\lambda_c + \lambda_r$
R_{cond}	=	Conductive resistance due to fouling
r_{i+1}	=	Outside radius with fouling mass
r_i	=	Original radius without fouling
k_i	=	Thermal conductivity of fouling media
R_{cond}	=	Convective resistance
h_o	=	Outside film coefficient
r_o	=	Outside radius
h_{new}	=	Equivalent heat transfer coefficient

METHODOLOGY

Analysis of the material on the ID of the corroded tubes indicated that sulfidation had occurred. Additionally, during the retubing operation, hard and soft scale fouling was detected on the OD of the tubes. It was hypothesized that the OD fouling led to higher internal temperatures and the resulting corrosion.

As a first step in analyzing the previous performance of the boiler, the historic operational data captured through the distributed control system (DCS) was examined. Several important process parameters (as described in the **INVESTIGATION OF PREVIOUS OPERATION** Section) were determined. These parameters were then used to determine the typical states of operation for the boiler during the 9 year service period. Process combustion analyses were then used to determine the fluid properties for integration into the process-side CFD models.

To determine the nominal tube operational temperatures, periodic CFD models were constructed of the original inlet ferrule design and of the multi-piece design installed during the retubing effort. Analyses were conducted using nominal process conditions to predict the heat fluxes and peak temperatures associated with the standard modes of boiler operation. As reported in the previous work [1, 2], there exists an area of recirculation downstream from the ferrules' termination where recirculating flow and high levels of turbulence increase the heat transfer from the process gas through the tube. The authors have found that CFD modeling is the only method that successfully predicts the peak fluxes and temperatures at this location.

The results of the CFD analyses were queried and a series of fits (as described in the **HISTORICAL TEMPERATURE AND CORROSION PREDICTION** Section) was performed. The fits were used to develop relationships to predict the peak tube temperature based on measured process data. These relations were incorporated into a MatLab (MathWorks [5]) routine. This routine used historical data captured through DCS to predict the peak tube temperature for the history of the boiler. Logic was then added to the MatLab routine to allow prediction of the corrosion rate, interpolated from Figure 1. The historical corrosion data was then integrated in time to determine the total expected corrosion of the tubes.

The CFD model of the original ferrule configuration was updated to allow the consideration of OD fouling resistances. A series of analyses was performed with various fouling factors to determine the peak ID temperature for a given fouled condition. A relationship was then derived between the OD fouling factor and the peak internal temperature. The MatLab routine was modified to allow prediction of the ID corrosion given different fouling growth regimes, based on the standard fouling growth equation. The routine was used to determine if the previous internal corrosion was due to singular operational events, or if it was more probable that the corrosion was a long-term phenomena.

It is known that kettle type boilers with buoyancy driven flow patterns are especially susceptible to FOC events. To determine the MOS to an FOC event, a 3-dimensional model was developed of the shell-side of the boiler. The results of the process-side CFD analyses were used to develop the heat flux boundary conditions for this model. Parameters from the previous work [1] were used to determine the MOS from a departure from nucleate boiling (DNB) event.

The results from the analyses were then combined to derive operational limit curves for the boiler based on plant measurable process parameters.

INVESTIGATION OF PREVIOUS OPERATION

It is known from historical boiler operational data and past investigations that several parameters are important to predicting the boiler's operation. These parameters with a brief description of their influence are:

1) Acid Gas Flow Rate – Primary influence on the mass flow through the boiler. At higher mass flows, the Reynolds number and downstream ferrule turbulence will increase, resulting in increased peak heat flux and tube temperature.
2) Acid Gas Composition – The acid gas composition will determine which reactions, other than the primary reactions, will occur. The nature of the reactions will influence the inlet temperature to the boiler.
3) Feed Rate x Inlet Temperature – This parameter - also referred to as pseudo-duty - provides an estimate of the boiler's duty. Both input quantities are measurable with typical plant process equipment.
4) O_2 Concentration – The maximum adiabatic combustion temperature will occur at an equivalence ratio of 1 (Babruaskas [6]). The concentration of O_2 for reaction with the process streams will control the equivalence ratio; hence, the temperature entering the WHB.

A review of the DCS archive data using the parameters above indicated 4 process points of interest: average air only case, maximum air only case, low CO_2 in the process gas case and maximum O_2 enrichment case. An additional case at 10% greater mass flow than the maximum O_2 case was also selected for analysis to determine the maximum tube fluxes and temperatures possible during a short-term plant excursion.

Process combustion analyses were performed on the cases to determine the properties required for the process CFD analyses. These gas properties include: mass flow rate, density, temperature, thermal conductivity, viscosity and specific heat.

PROCESS SIDE CFD ANALYSIS

To perform the process side CFD analyses, 1/12th periodic models were developed of the ferrule/tubesheet/tube intersection for both ferrule geometries under consideration. The model domains included: gas, tube, tubesheet, Kaowool wrap, the ferrule, Kaowool insulating board, Greencast refractory and the hex refractory. Figure 3 highlights the domains considered for the original ferrule geometry analysis.

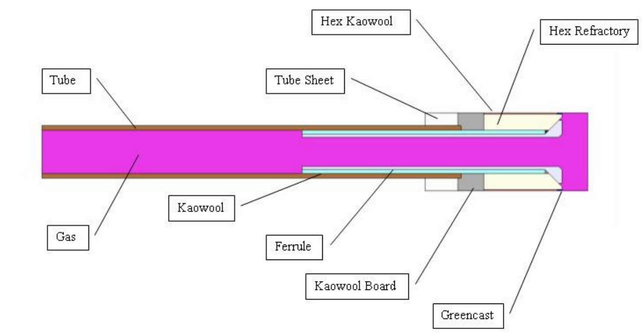

FIGURE 3 – DOMAINS USED FOR PROCESS SIDE CFD ANALYSIS

Structured computational grids were developed for the models' domains. As the heat transfer from the gas to the tube was critical in the analyses, significant near-wall refinement was employed during grid development. The final computational models each contained approximately 600,000 computational cells with ¾ of the cells used for the fluid (gas) domain. The authors have developed many grids for various inlet geometries in this region of WHBs and have developed a gridding technique that allows for the capture of all relevant flow and heat transfer mechanisms in the region. Figure 4 shows a sample computational grid used for the analyses.

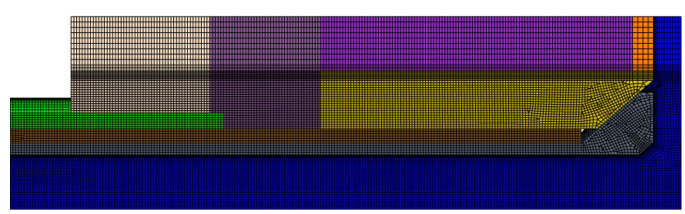

FIGURE 4 – STRUCTURED GRID USED FOR CFD ANALYSIS

Steady-state analyses were performed for the 5 process conditions (described in the **INVESTIGATION OF**

PREVIOUS OPERATION Section) in Star-CCM+ v. 4.06 (Adapco [7]). The process gas was treated as incompressible since the gas properties do not significantly change in the area of interest, and turbulence was included through the use of the RNG k-ε turbulence model with low Reynolds number and all Y+ values considered. This model provides the best results when Y+ values are below 50 [4]. Due to the near-wall resolution of the boundary layer all Y+ values in the areas of interest were below 4.

Radiation was included through the discrete ordinate (DO) radiation model. The DO model traces rays from the centroid of each participating cell through the domain to determine the view factors between cells. The quadrature of the model determines the number of rays traced. For these analyses, the S8 quadrature (8 rays per cell) was used. Standard radiation theory is combined with the calculated view factors to determine the radiative fluxes in the model.

The tube and tubesheet steel were modeled as an isotropic material with a standard thermal conductivity of 28 BTU/hr*ft*°F (ASME [8]). Polynomial functions were used to model the thermal conductivity of the Kaowool and refractory based on vendor-supplied properties (Thermal Ceramics and Harbison-Walker respectively).

As expected, recirculation regions do exist downstream from the ferrule. The recirculation results in a maximum tube heat flux and a correspondingly high temperature. This recirculation region is shown in Figure 5.

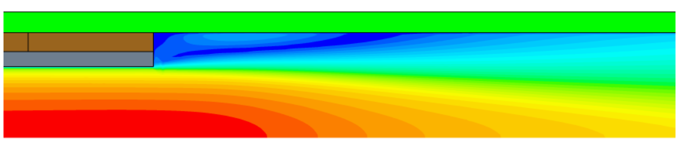

FIGURE 5 – VELOCITY MAGNITUDES DOWNSTREAM FROM FERRULE TIP

HISTORICAL TEMPERATURE AND CORROSION PREDICTION

Queries were made of the peak heat flux and tube temperature analysis results from the periodic CFD analyses for both models. It was known that the maximum flux occurring downstream from the ferrule should be related to the pseudo-duty. Therefore, a plot of these two parameters was constructed, as shown in Figure 6.

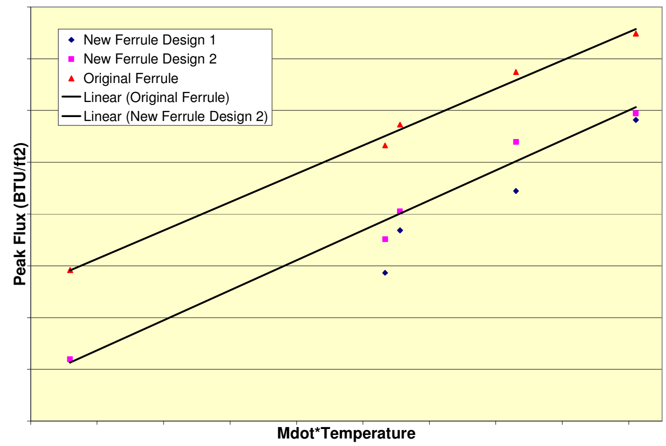

FIGURE 6 – PEAK FLUX VERSUS PSEUDO-DUTY

Clearly, there exists a linear relationship between the peak flux predicted by the CFD analyses and the pseudo-duty. The difference between the peak flux line for the old and new ferrule designs is due to a change in the ferrule termination in the new design resulting in less recirculation. This flux variation - based on geometric differences - has been observed in other analyses conducted by the authors.

Several fit types were used to determine a relationship between the peak flux and the peak tube temperature. Basic thermodynamics stipulates that there should be a linear relationship between these variables, because the system simplifies to a conductive problem through a known thermal resistance (the tube). Scatter existed in the data when this linear fit was performed, as shown in Figure 7.

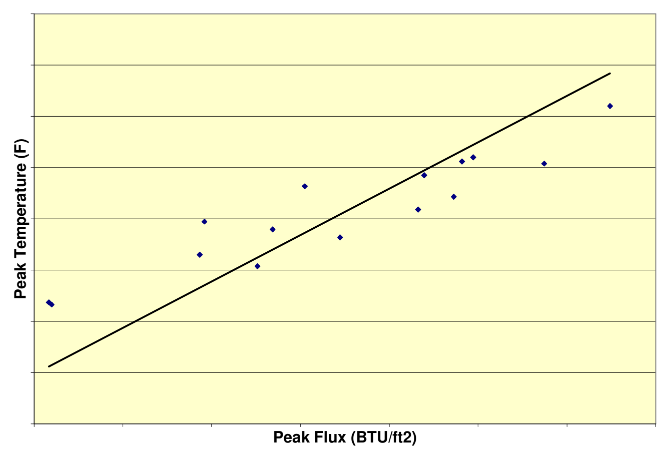

FIGURE 7 – PEAK TEMPERATURE VERSUS PEAK FLUX

For this reason it was decided to perform a second fit of the ratio of the peak temperature / peak flux versus the peak flux. This fit represents the derivative of the linear function described above and would be expected to have a slope of zero. The fit of these variables is shown in Figure 8.

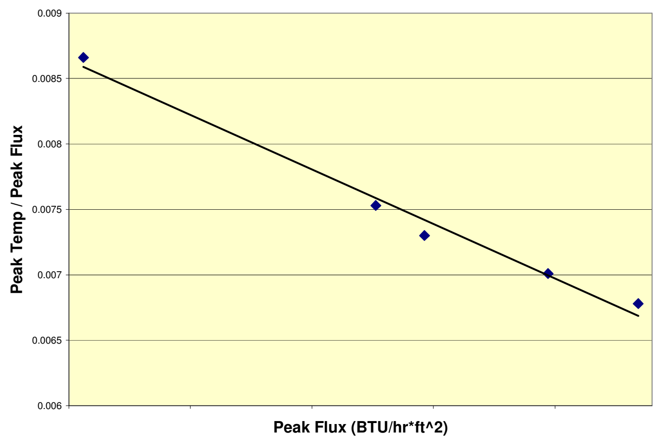

FIGURE 8 – PEAK FLUX VERSUS PEAK TEMPERATURE / PEAK FLUX

Due to confidentiality agreements, the peak flux values cannot be presented in this paper, but it can be seen that a good linear correlation exists between the data. It can also be seen from the change in the ordinate axis that the slope of this line is nearly 0 (~ $1x10^{-8}$), as would be expected. As this fit provided better correlation and could be implemented through numerical integration, it was chosen for predicting the peak tube temperature.

A MatLab [5] routine was developed to allow the prediction of the peak tube temperature based on historical operation data. This routine read the volumetric flow rate in MMSCFD, whether the feed stream was reacted with extra oxygen, the inlet pressure and temperature from an Excel database with historical data at 1 hour periods. It was known for this process that the gas had a molecular weight (MW) of 26.65 when not reacted with extra oxygen and 26.5 when reacted with extra oxygen. The routine used the data above to convert the volumetric flow rate in MMSCFD to MMACFD. From this information a mass flow rate was determined for the time step. The product of the mass flow rate and the inlet temperature was used to predict the peak flux using the relations shown in Figure 6. The rate of change of the tube temperature was then computed using the relation in Figure 8. This was then time-integrated to find the tube temperature. Figure 9 shows the temperatures predicted from the operational data.

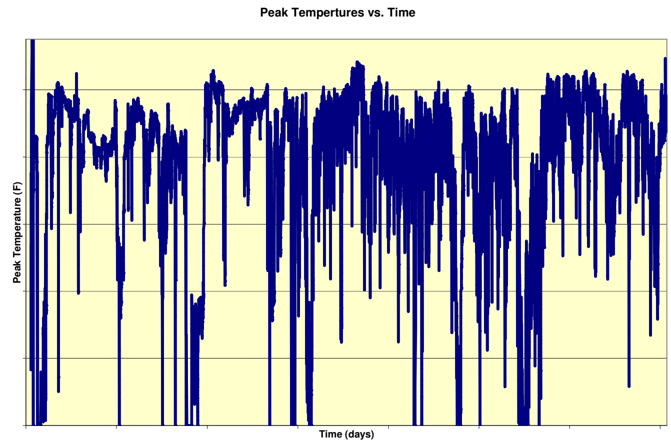

FIGURE 9 – PEAK TEMPERATURE VERSUS TIME

The MatLab temperature routine was expanded to predict the expected in-service corrosion based on Figure 1. To implement the corrosion function, the predicted temperature at the time point was used to find a corresponding corrosion rate with an assumed H_2S concentration of 4 %Mol. The corrosion value was then integrated over time to find the total corrosion for the step. The results of this analysis indicated that no more than 35 mils of corrosion would be expected from the data without a secondary mechanism.

CONSIDERATION OF OD FOULING

Inspection of the OD of the tubes during the retubing operation indicated the presence of hard and soft scales on the tube OD. It is known that the presence of a scale will increase the conductive thermal resistance across the tube, increasing the ID temperature. The fouling resistance caused by scaling is highly dependent on crystalline packing fractions in the deposits as well as their compositions (EPRI [9]). Consequently, estimates based purely on chemical analysis of the removed scale are not reliable for predicting the fouling factor and their resistance is most commonly characterized through physical testing. As it was impossible to remove the tubes without disturbing the soft scale, no lab measurement could be made of its thermal conductivity/fouling resistance. Therefore, to provide guidance for future operations it became necessary to determine the effect of varying fouling resistances on the maximum internal tube temperature. Specifically, a determination was required as to whether the corrosion was caused by singular operational events or if it was caused by long-term operation.

Determining the corrosion regime required modifying the MatLab program to account for the additional thermal resistance provided by the external fouling. As no information for the thermal conductivity of the fouling (evidenced during retubing) was available, the modified program would be used to back-solve the fouling resistances required to achieve the in-service corrosion. The magnitude of the fouling resistance could then be used to determine the fouling regime.

Research on fouling mechanisms (Turner [10]) indicated that the fouling mass can be modeled through the fouling growth equation.

$$m(t) = \frac{k\rho}{\lambda}\left(t\lambda_c + \frac{\lambda_r}{\lambda}\left(1 - e^{-\lambda t}\right)\right) \tag{2}$$

Inspection of the equation shows that - depending on the choice of the consolidation and deposition rate constants - the fouling mass can grow linearly, asymptotically or can decrease over time. For the WHB, the condition of decreasing fouling over time can be neglected. It should be noted that for the purposes of this investigation, Equation 2 can be simplified by combining κ, ρ and λ into a constant (the constant). Next the fouling mass was assumed to distribute evenly over the outside of the tube. In this case the increase in mass (volume) can be assumed to vary as the square of the external fouling radius. The resistance across the fouling could then be predicted using basic thermodynamics, where $r_{i+1} \sim m(t)^{0.5}$, and k_i can be combined with the constant (Hodge [11]).

$$R_{cond} = \frac{\ln(r_{i+1} - r_i)}{2\pi * k_i} \tag{3}$$

The shell-side convective resistance is known to be:

$$R_{conv} = \frac{1}{h_o 2\pi * r_{o`}} \tag{4}$$

The combined resistance is the sum of Equations 3 and 4. This combined resistance can then be used to solve for an effective external convective coefficient:

$$h_{new} = \frac{1}{2\pi * r_{i+1}\left(R_{cond} + R_{conv}\right)} \tag{5}$$

The effective film coefficient can be determined as a function of time using Equations 2 – 5, as shown in Figure 10.

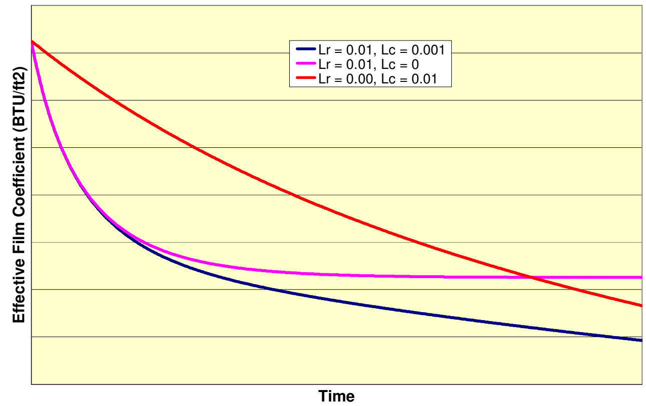

FIGURE 10 – EFFECTIVE FILM COEFFICIENT VERSUS TIME

It was necessary to relate the effective coefficient to the peak internal tube temperature to determine the fouling resistance's effect on tube corrosion. To determine this relationship, the original periodic CFD models were updated to allow modification of the water side convection coefficient downstream of the ferrule. A series of analyses was then performed to determine the effect of reduced external film coefficients (increased system thermal resistance) on the internal tube temperature. A review of the data showed that a power law relationship could be derived between the inverse of the increase in tube temperature and the reduction in film coefficient, as shown in Figure 11.

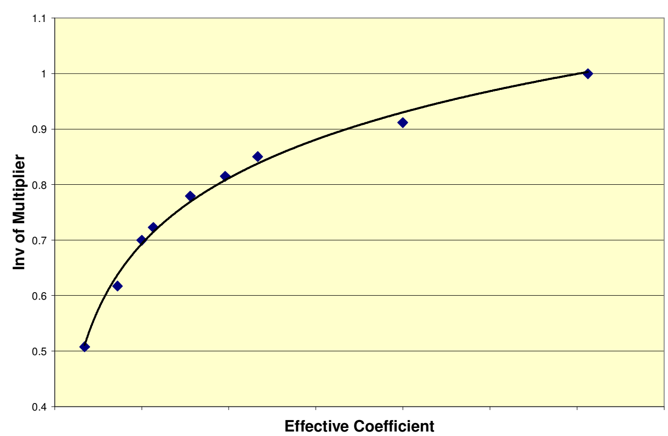

FIGURE 11 – INVERSE TEMPERATURE MULTIPLIER VERSUS FILM COEFFICIENT

The effective coefficient versus time could then be combined with the relationship in Figure 10 to determine an internal tube temperature multiplier versus time as shown in Figure 12.

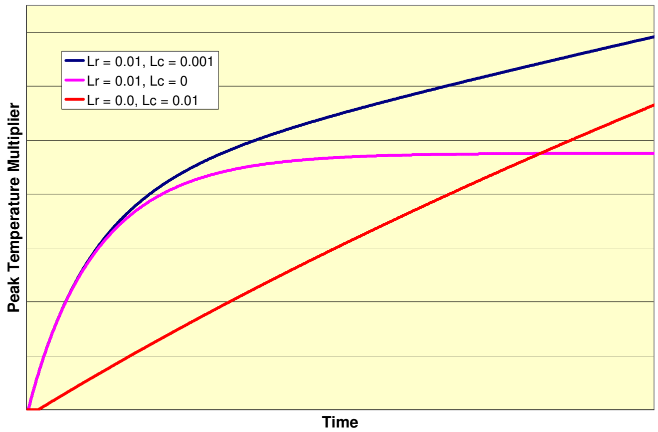

FIGURE 12 – TEMPERATURE MULTIPLIER VERSUS TIME FOR ASSUMED FOULING REGIMES

The MatLab routine was updated to allow consideration of these fouling growth regimes. A series of analyses was conducted to determine the most likely tube fouling candidate (linear or asymptotic mass growth) or singular fouling events. This determination was made by solving for a constant required to meet the tube corrosion discovered on inspection. The multiplier could then be used to determine the thermal resistance / fouling factor versus time. It was found that the final values of the thermal resistance for both the linear and asymptotic growth assumptions were within 5% of each other and low enough that the fouling should not be detected with typical process measurements. While the final value of the external fouling factor was approximately 10 times the design basis factor, significant fouling only occurred over approximately 2% of the total heat transfer area, resulting in no detectable change in the total exchanger heat transfer duty. Figure 13 shows the cumulative corrosion caused by asymptotic fouling growth.

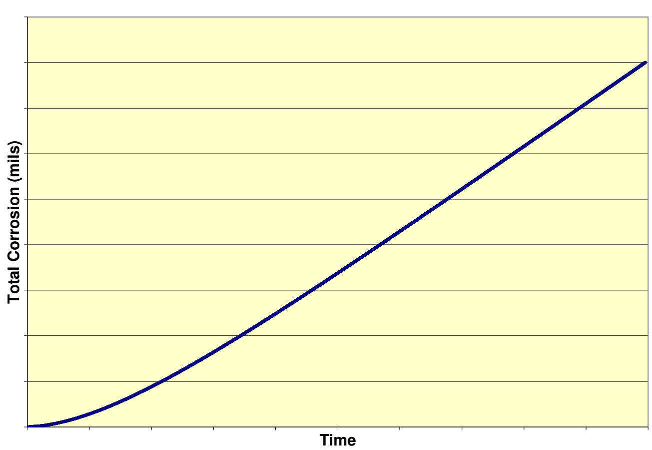

FIGURE 13 – CUMULATIVE CORROSION VERSUS TIME FOR ASYMPTOTIC FOULING GROWTH

An additional analysis was conducted in which the fouling factor was step-increased 4 times over the operational time span. Assuming the fouling was caused by singular events, it was determined that the magnitude change of the thermal resistance - if the corrosion was caused by singular events - would lead to a fouling factor great enough to be detected in process measurements. Therefore, it could be reasonably stated that the corrosion was due to ongoing fouling within the WHB where the mass grew linearly or asymptotically over the time period and was not caused by singular events. The intermittent blow-down had not operated during the 2000 – 2009 period, so it was recommended that steps be taken to periodically operate the blow-down during future operations. It was also recommended that shell-side inspections for fouling be conducted when the boiler is serviced in the future.

3D SHELL-SIDE CFD MODELING

To quantify the FOS between the boiler's normal operation and an FOC event, a 3D CFD analysis of the shell-side of the boiler was performed. During an FOC event, the nucleating bubbles on the boiler's tubes fail to depart in jets and columns, coalescing into bubbles. This is also known as a DNB event. Instead, a steam film forms over the heating surface transforming the primary heat transfer mode from convection to a fluid (water) to convection to a gas (steam), causing a significant temperature rise while limiting the peak flux that can be conducted through the tube. Lienhard [12] has shown that this phenomenon is conditionally stable. Model parameters that can be used to determine if an FOC event will occur include the wall superheat, the local wall steam volume fraction and the peak wall heat flux. Critical points for these values are extensively discussed in a previous paper [1].

To conduct the CFD analysis, a model was constructed of the first 30" on the first pass of the boiler, including the tubes. The second pass was approximated through the use of a porous media. The computational grid was constructed using a structured grid with near wall refinement in the vicinity of the tubes. The model used for analysis contained 24.7 million computational cells and is shown in Figure 14.

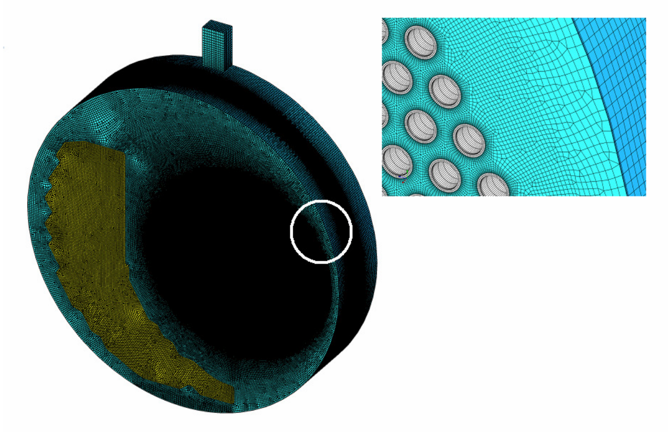

FIGURE 14 – 3D MODEL USED FOR SHELL-SIDE CFD ANALYSIS

The shell-side fluid was modeled using a volume of fluid (VOF) physics model with boiling included. The VOF model assumes the fluid phases on the shell-side (steam and water) are immiscible. The boiling model tracks the production and volume fraction of steam on a cell-by-cell basis. Fluxes from the maximum periodic flux case were applied to the inside of the tubes through the use of X, Y, Z table data created using a MatLab function. Two cases were considered, one with a clean external tube and one with a fouling resistance on the outside of the tube. The second case was performed to ensure that water side fouling would not initiate an FOC event.

The results of the analyses indicated that volume fractions on the outside of the tubes approach the limiting fractions used by the nuclear industry for a DNB event (Reisch [13]). The peak heat flux and wall superheat temperatures indicated an adequate MOS to the FOC event. Due to the high velocities occurring in the boiler (shown in Figure 15), it is believed that the high volume fraction locations were not stable.

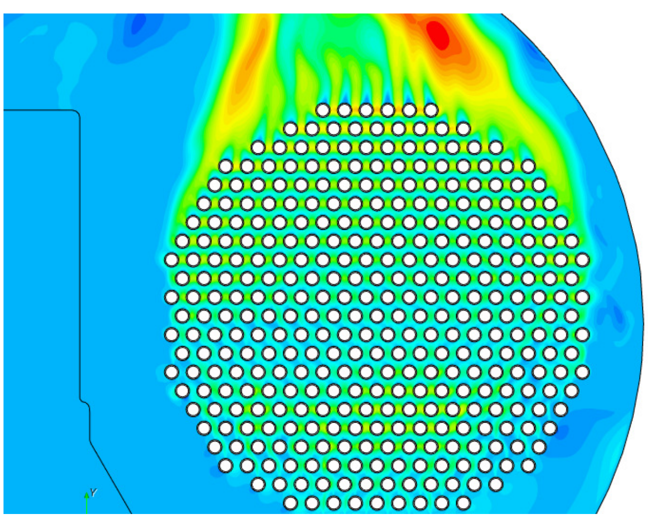

FIGURE 15 – SHELL-SIDE BUNDLE VELOCITES

It was hypothesized that the high velocities within the bundle were due a comparatively long flow path through the bundle (355 tubes) versus previously analyzed bundles (150 – 200 tubes).

OPERATIONAL CURVE DEVELOPMENT

For the boiler under consideration, there are two possible failure modes: a) long-term sulfidation corrosion caused by high tube temperatures, and b) short-term failure caused by a FOC event, or over-temperature of the refractory. Both of these conditions must be considered when determining the operational limits of the boiler. Additionally, any operational limit curve must use process information routinely measured in the plant, specifically process flow and inlet temperature.

Review of the temperature results from the periodic CFD analyses indicated that, due to the as-built design, the peak tube temperature would occur at the tube-to-tubesheet weld. The results of the analyses, as discussed in the **HISTORICAL TEMPERATURE AND CORROSION PREDICTION** Section, were queried and a new linear fit was performed on the temperature data at the tube-to-tubesheet weld location, as shown on Figure 16.

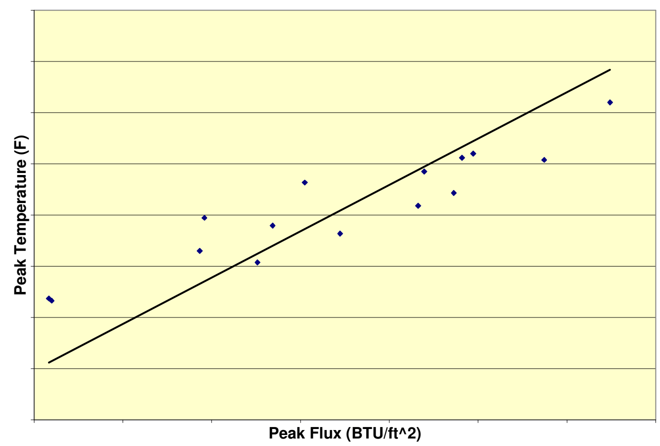

FIGURE 16 – PEAK TUBE TIP TEMPERATURES VERSUS PEAK FLUX

The MOS calculated during the 3D shell-side analysis was combined with the peak flux versus pseudo-duty curve shown in Figure 5 to determine a relationship between the inlet mass flow and temperature. This curve is limiting for a short-term plant excursion until the thermal reactor firing temperature reaches the allowable temperature for the refractory. The refractory over-temperature condition is limiting at all mass flows.

Using the information above, two operational curves for the boiler can be developed, as shown in Figure 17.

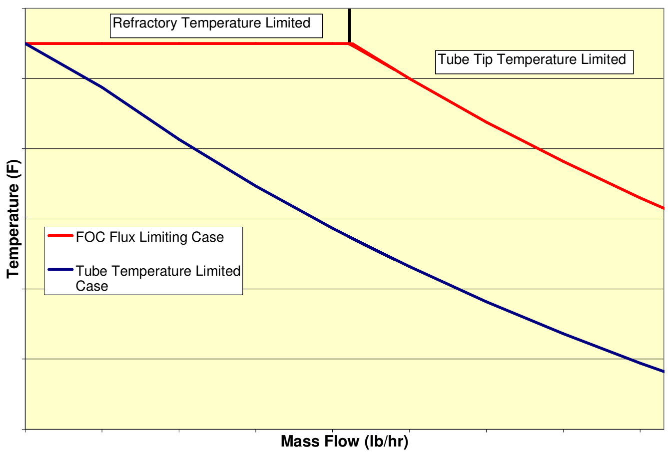

FIGURE 17 – OPERATIONAL LIMIT CURVES

The limit represented by the blue line is the long-term operational limit for the plant. The red line represents the limit for short-term plant process excursions through either refractory over-temperature or an FOC event leading to short-term mechanical failure of the tubes. Exceeding this limit may result in equipment failures necessitating a plant shutdown.

It should be noted that these curves are usually derated from the maximum values calculated through numerical analysis based on the level of confidence in the numerical analysis and the plant's ability to accurately measure process data.

CONCLUSIONS

This paper presents methodologies for the use of data derived through CFD and empirical analyses to extrapolate several characteristics related to the long-term operation of a WHB. These include the ability to predict operational temperatures based on DCS historical data, the ability to predict fouling regimes based on the fouling growth equation [10], and the ability to derive operational limit curves for both long-term corrosion and short-term FOC or refractory over-temperature events. Specifically, the analyses presented in this paper demonstrated that the tube corrosion did not occur due to an FOC event and that it instead occurred over a long period of time due to external corrosion.

Analyzing the WHB's performance over a 9 year operational cycle would have been impossible with a transient CFD model. However, combining the data derived from simplified CFD analyses with sound engineering judgment provided the information necessary to derive significant data for future WHB operations. This data was then used to develop short-term excursion and long-term process parameters for the WHB's operation. The analyses were also able to produce future operational guidance related to the use of the intermittent blow-down and shell-side inspections.

It should be noted that the procedures and analyses detailed in this paper are not the complete analyses performed to qualify the past performance of the boiler and to determine the boiler's operational limits. Complete engineering to determine these limits requires additional analyses.

AKNOWLEDGEMENTS

The authors would like to thank Thomas Hirst for his assistance preparing data for the graphs in the paper.

The authors would also like to thank KPS Technology & Engineering for the reduction and preparation of the DCS historical operational data, and for conducting the process-side combustion analyses.

REFERENCES

[1] Porter, M., Martens, D., McGuffie, S., Wheeler, J., 2009. A Means of Avoiding Sulfur Recovery Reaction Furnace Fired Tube Boiler Failures. PVP2009-78073

[2] Porter, M. Martens, D., Duffy, T., McGuffie, S., 2005. Computational Fluid Dynamics Investigation of a High Temperature Waste Heat Exchanger Tube Sheet Assembly. PVP 2005-71143

[3] Siemens, 2007. Process Analytics in Claus Plants, Case Study.

[4] CD-Adapco, Star-CCM+ Users Guide, How do I decide on a wall treatment?

[5] The MathWorks, Inc. 2007. MatLab, v. 7.5.0.342 (R2007b)

[6] Babruaskas, V., 2006. Temperatures in Flames and Fires. Fire Science and Technology, Inc.

[7] CD-Adapco, Star-CCM+, v. 4.06

[8] ASME, 2007. 2007 ASME Boiler and Pressure Vessel Code. Section II, Materials. New York, NY

[9] EPRI, Steam Generator Thermal Performance Degradation Case Studies, Report TR-110018, Palo Alto, CA

[10] Turner, C., Klimas, S., 2001. Modeling the Effect of Surface Chemistry on Particle Fouling Under Flow-Boiling Conditions. Proceeding of Heat Exchanger Fouling: Fundamental Approaches and Technical Solutions. AECL Report 12171

[11] Hodge, B.K. 1990. Analysis and Design of Energy Systems, Second Edition. Prentice-Hall, Inc. Englewood Cliffs, NJ.

[12] Lienhard, J., IV, Lienhard, J. V, 2008. A Heat Transfer Textbook, Third Edition. Phlogiston Press. Cambridge, MA

[13] Reisch, F., 2006. Dryout of BWR Fuel Elements, Nuclear Power Safety. KTH Royal Institute of Technology. Stockholm, Sweden